

Shielding Properties of Cement Composites Filled with Commercial Biochar

Original

Shielding Properties of Cement Composites Filled with Commercial Biochar / Yasir, M.; di Summa, Davide; Ruscica, Giuseppe; Natali Sora, Isabella; Savi, Patrizia. - In: ELECTRONICS. - ISSN 2079-9292. - (2020), pp. 1-10. [10.3390/electronics9050819]

Availability:

This version is available at: 11583/2825972 since: 2020-05-16T19:59:48Z

Publisher:

MDPI

Published

DOI:10.3390/electronics9050819

Terms of use:

openAccess

This article is made available under terms and conditions as specified in the corresponding bibliographic description in the repository

Publisher copyright

(Article begins on next page)

Article

Shielding Properties of Cement Composites Filled with Commercial Biochar

Muhammad Yasir¹, Davide di Summa², Giuseppe Ruscica², Isabella Natali Sora², Patrizia Savi^{1*}

¹ Dept. of Electronics and Telecom., Politecnico di Torino, C.so Duca degli Abruzzi 24, 10129 Torino; Italy

² Dept. of Engineering and Applied Sciences, Università di Bergamo, Dalmine; Bergamo; Italy

* Correspondence: patrizia.savi@polito.it

Received: date; Accepted: date; Published: date

Abstract: The partial substitution of non-renewable materials in cementitious composites with eco-friendly materials is promising not only in terms of cost reduction, but also in improving the composites shielding properties. The water and carbon content of a commercial lignin-based biochar is analyzed with thermal gravimetric analysis. Cementitious composites samples of lignin-based biochar with 14wt.% and 18wt.% are realized. Good dispersion of the filler in the composites are observed by SEM analysis. The samples are fabricated in order to fit in a rectangular waveguide for measurements of the shielding effectiveness in X-band. A shielding effectiveness of 15dB was obtained at a frequency of 10GHz in the case of composites with 18wt.% of biochar. Full-wave simulations are performed by fitting the measured shielding effectiveness to the simulated shielding effectiveness by varying material properties in the simulator. Analysis of the dimensional tolerances and thickness of the samples is performed by the help of full/wave simulations. Lignin-based biochar is a good candidate for partial substitution of cement in cementitious composites as the shielding effectiveness of the composites increase substantially.

Keywords: shielding effectiveness; biochar; eco-friendly material; cementitious composites; waveguides.

1. Introduction

The human population has seen rapid growth in the past decades. With increasing population, the demand for construction industry has increased manifold [1]. This has resulted in increasing greenhouse gas emissions from cement production [2]. The substitution of non-renewable raw materials used in construction industry with eco-friendly materials derived from waste is promising in terms of cost and environmental protection [3]. Agriculture and forestry waste is primarily burnt on field in order to reduce the cost of disposal. When converted into biochar, this waste can be used as a partial substitute to cement resulting in a significant reduction in greenhouse gas emissions and improving the mechanical properties of concrete [4,5].

Increasing number of devices working at microwave and millimetre wave frequencies has resulted in an overall increase in electromagnetic radiation [6,7]. Electromagnetic shields are deployed to protect sensitive devices against electromagnetic interference [8,9]. In places that are vulnerable to electromagnetic interference, shielding materials can be applied as a coating on wall surfaces [10]. A number of equipment working at microwave and millimetre wave is used in the health sector for applications like imaging, tomography etc. [11,12]. The X-band is particular is important for radar communications including air-traffic control, weather monitoring, maritime vessel traffic control, defence tracking, vehicle speed detection. The use of shielding materials in building can be helpful in isolating equipment that is sensitive to electromagnetic interferences [13,14]. Different measurement techniques can be deployed for the determination of shielding effectiveness of materials. The most common measurement techniques are reverberation chamber [15], free-space measurements in

anechoic chamber [16], coaxial and waveguide methods [17-19]. Each measurement technique requires specific samples dimensions and frequency band. The X-band is very important for applications like, satellite communications and radar.

The use of carbon based materials in epoxy composites and the analysis of their morphological and electrical properties has been vastly studied [20-23]. Conventional carbon based materials like graphene and carbon nanotubes are expensive and require a complex synthesis. In recent years, the use of biochar substituting carbon nanotubes and graphene in composites as filler is investigated [24-25]. Biochar is cost effective as compared to other carbon based materials. Biochar is a porous carbonaceous material produced by thermal treatment of biomass in absence of oxygen [26]. It can be made from a number of different waste products such as agricultural, food waste or sewage sludge [27]. Until recently biochar has been used for soil amendment in agriculture and landfilling applications [28]. The use of biochar in alternative applications is being studied at a vast scale, specifically for carbon sequestration, energy storage applications [29] and in construction and building [30-31].

In this paper, lignin-based commercial biochar is used as a partial substitute to cement in composites. The water, carbon and other residues of the biochar is studied by TGA. Composites of 4mm thickness with plain cement, 14 wt.% biochar and 18 wt.% biochar are fabricated with specific dimensions for measurements of the shielding effectiveness inside a waveguide working in the X-band microwave frequency. The sample with 18 wt.% biochar were cured in water for 7 days or 28 days. For examining the microstructural properties of the composites and dispersion of the filler in the composite matrix, SEM is adopted. Measurements of the shielding effectiveness are compared with simulated results obtained with a full-wave simulator. As expected the shielding effectiveness increases with the increase of the percentage of filler (11dB for 14wt.%, and 15dB for 18wt.% at 10GHz). Analysis of fabrication tolerances and sample thickness are performed by the help of a full-wave simulator.

Finally, the effect of the curing period in water on the shielding effectiveness values is analysed for the samples with 18wt.% biochar. The shielding effectiveness increases by approximately 5dB in the whole frequency range for the sample cured in water for 28 days with respect to the sample cured in water for 7 days.

2. Materials and Methods

2.1. Composites preparation

The composite samples produced are with 14wt. % and 18 wt.% of biochar in Portland cement. For the sake of comparison, a composite without biochar is also produced, which is referred to as plain cement composite. The biochar used to realize the samples is a commercial product provided by Carlo Erba Reagents. It is pyrolysed in the form of powder at a temperature of 750 °C for four hours in an alumina crucible. For preparation of cementitious composites ordinary Portland Cement (PC) (grade 52.5 R) compliant with ASTM C150 is used along with water and superplasticizer to form an adequate consistency of the paste. The percentages of water and superplasticizer used are equal to 60 wt.% and 1.8 wt.% respectively. A mechanical mixer is used to work the mixture for a duration of 5 minutes. Silicon moulds of adequate shape and size are then used to give the composites the required shape and dimensions.

Portland cement is blended with biochar by using a mechanical mixer for 5 minutes with two different percentages by weight of cement, 14% and 18%, water (60%) and superplasticizer (1.8%). Furthermore, a reference specimen is realized using only Portland cement matrix blended together with a water and superplasticizer equal to 35% and 1.5%. The obtained composite are then poured into rectangular silicone moulds for shielding effectiveness analysis. The silicone moulds are fabricated in a 3D printed

master mould of specific dimensions (see Figure 1). The reusable and flexible silicone moulds helps in easy extraction of composite samples once they are cured.

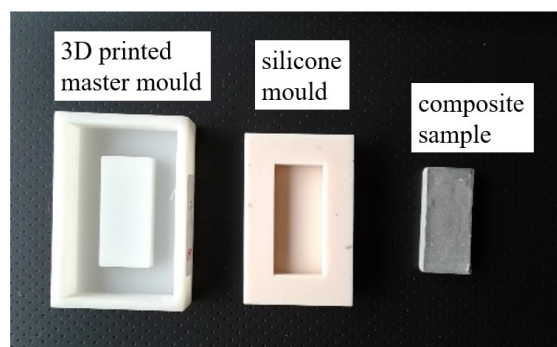


Figure 1. 3D printed master mould with silicone mould and an example of composites.

Initially, the composite samples are kept at a relative humidity of $90 \pm 5\%$ for 24 hours. The composites are then demoulded and immersed in water at a temperature of $20 \pm 2^\circ \text{C}$. The samples are then cured in water for a period of 7 days. Two different curing methodologies are used for curing of the 18wt.% samples in water for 7 days and 28 days in order to evaluate the impact of water curing duration on the shielding effectiveness (see Table 1). In Table 1 the different steps of fabrication and measurements of the cement composites are reported.

Table 1. Fabrication and measurements of the cement composites.

Day	Plain cement	14 wt. % (7 days)	18 wt.% (7 days)	18wt.% (28 days)
0	fabrication	fabrication	fabrication	fabrication
1	demoulded	demoulded	demoulded	demoulded
1	cured in water	cured in water	cured in water	cured in water
7	extracted from water	extracted from water	extracted from water	--
21	SE meas. 2 weeks	SE meas. 2weeks	SE meas. 2 weeks	--
28	--	--	--	Extracted from water
42	--	--	--	SE meas. 2 weeks
70	SE meas. 10 weeks	SE meas. 10 weeks	SE meas. 10 weeks	--
98	--	--	--	SE meas. 10 weeks

2.2 Morphological analysis

Thermogravimetric analyses TG-DTA analysis is carried out in air using about 20mg of biochar heated from room temperature to 950°C at $3^\circ \text{C}/\text{min}$. For a morphological characterization of the cement composites, a scanning electron microscope (Hitachi S-2500C) was used for the analysis of the cross section of cement composites with 18 wt.% biochar. Sections of the composite are cut and polished with measurements performed on gold plated samples to avoid any charging effects.

2.3 Radiofrequency measurements

The total shielding effectiveness can be defined as the ratio of the incident and transmitted field. It can be obtained from the measured transmission loss (S_{21}), in a waveguide as:

$$SE = -20 \log(|S_{21}|) \quad (1)$$

The total shielding effectiveness of a material comprises of dissipation loss, L_D , and mismatch loss, L_M [32]:

$$SE = L_D + L_M \quad (2)$$

where L_M can be calculated from the reflection scattering parameter by:

$$L_M = -10 \log_{10}(1 - |S_{11}|^2) \quad (3)$$

$$L_D = -10 \log_{10} \left(\frac{|S_{21}|^2}{1 - |S_{11}|^2} \right) \quad (4)$$

The scattering parameters of the composites are measured in a WR90 rectangular waveguide from 8GHz to 12GHz using a setup similar to [33]. The samples are fabricated in order to fit the rectangular waveguide cross section ($a=22.86\text{mm}$, $b=10.16\text{mm}$). The thickness of the samples is 4mm. The setup is shown in Figure 2. It consists of a two-port Vector Network Analyzer (VNA) (Agilent E8361A); two coaxial cables connected to the two ports of the network analyzer; two coaxial to waveguide adapters and two rectangular waveguides. Between the waveguides flanges is inserted a spacer holding the sample. Before the measurements, a two-port calibration (short, matched load, thru) is performed. The reference planes are at the ends of the spacer.

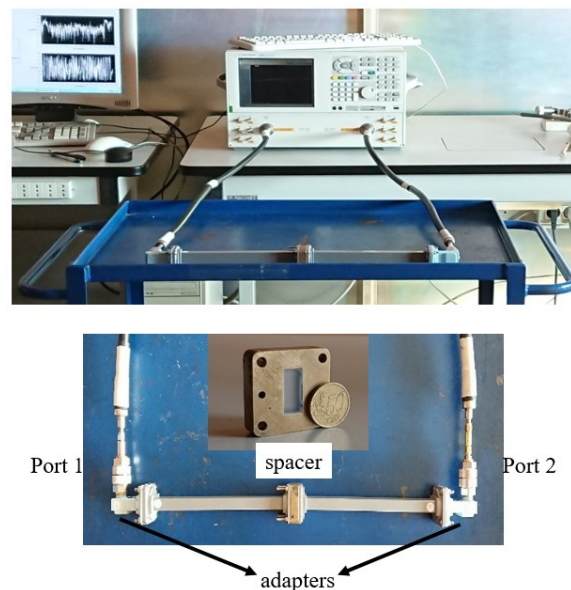


Figure 2. WR90 waveguide measurements setup.

2.4 Finite element simulations

A commercial finite element modelling tool, Ansys HFSS is used to simulate the waveguide with the composite sample as shown in Figure 3. The material properties of the composite inserted in the waveguide are chosen by fitting the simulated shielding effectiveness values to the measured shielding effectiveness values. The composite dimensions and thickness are varied to analyze the impact of fabrication tolerances and thickness on the values of shielding effectiveness.

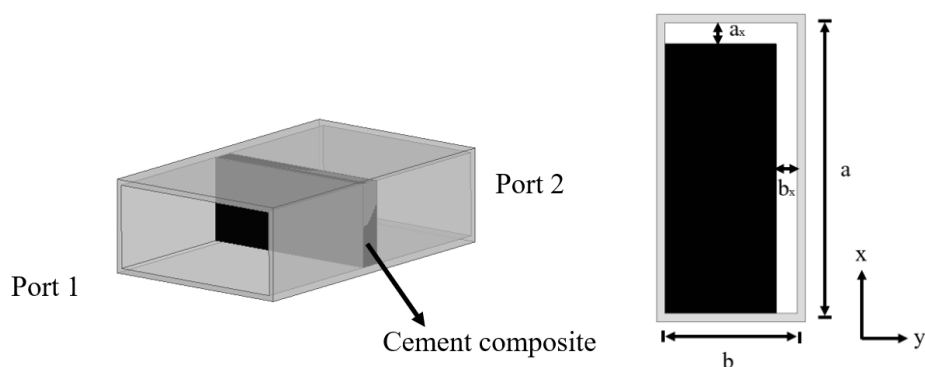


Figure 3. Geometry of the simulated waveguide with composite (left panel). Geometry for the dimensional analysis (right panel).

2.5. Dimensional tolerance analysis

In order to take into account the dimensional tolerance of the cement composite, simulations were performed based on varying the two dimensions along the x and y axis (see Figure 3). In case of plain cement composites, it was found that there is negligible variation of the transmission properties by varying the a_x dimension of the sample, while the impact of a variation of b_x is significant. A variation of 0.5 mm in b_x results in a variation of almost 1 dB in the transmission coefficient as shown in Figure 4. It has been ensured that the tolerance in the dimensions of the cement composites is below this value.

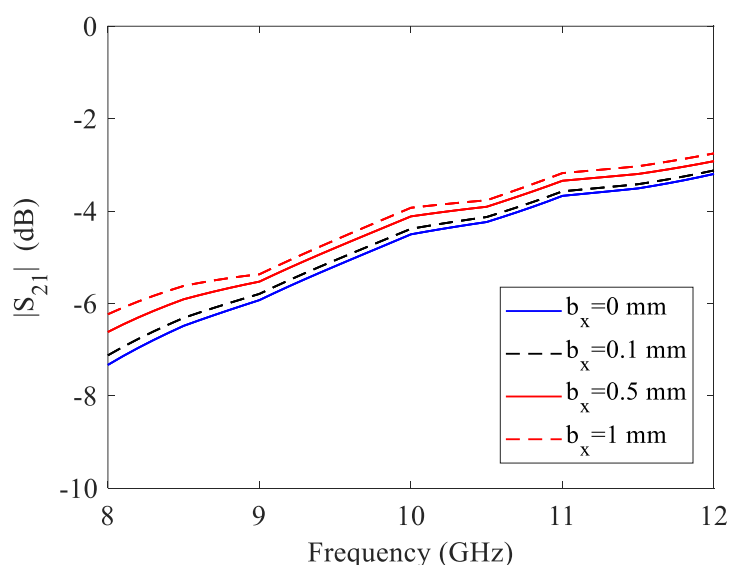


Figure 4. Analysis of fabrication tolerances of the plain cement composites.

3. Results

3.1. Biochar and composites characterization

The water and carbon content of the biochar is investigated by TG-DTA experiments. TGA curve of biochar is reported in Figure 5. Below 100 °C, the weight loss is about 16%, due to the evaporation of the physically adsorbed water. From 350 °C to 500 °C the weight loss is due to the combustion of the graphitic carbon fraction (about 74% of the total weight of the sample). At 950 °C, a residue of around 5 % in weight is observed respect to the initial amount.

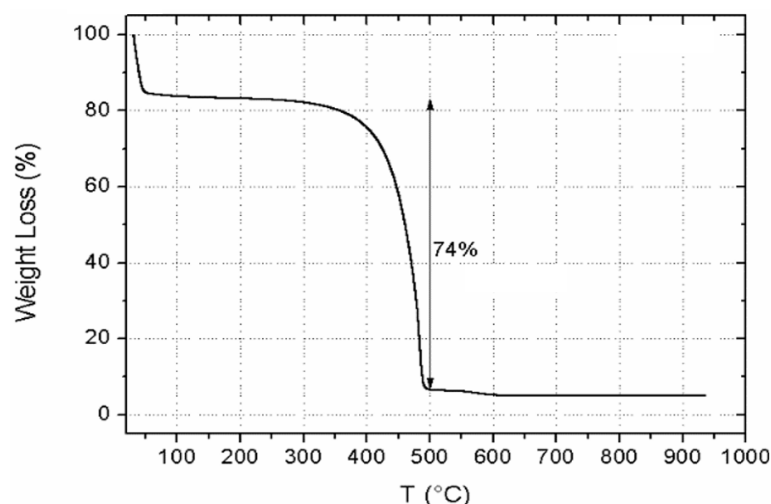


Figure 5. TGA curve of biochar filler.

Figure 6 illustrates the SEM image of composites with the highest content of biochar (18wt.%) recorded with secondary electrons. The black structures shown in the SEM image are the carbonaceous particles. The expected elongated structure of the particles is due to the fiber origin of the biochar. The particles show a good dispersion in the matrix.

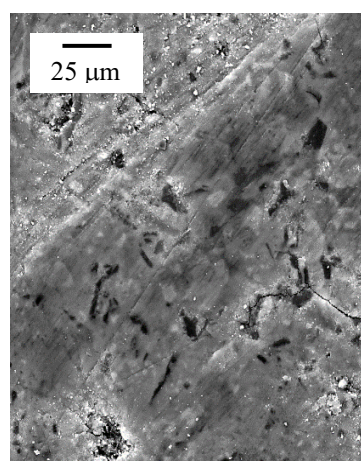


Figure 6. SEM Micrograph of cement containing biochar 18% at 1000x magnification.

3.2 Shielding effectiveness analysis

Shielding effectiveness can be found from the measured transmission coefficient, S_{21} , in a waveguide (see Figure 2) as defined in equation (1). The measured shielding effectiveness of the plain cement used as reference sample, sample with 14wt.% and 18wt.% filler cured in water for 7 days and measured after 10 weeks are shown in Figure 7. At the center frequency of 10GHz, the shielding effectiveness of plain cement is almost 5dB, which increases to 11dB for the samples with 14wt.% of biochar. The maximum shielding effectiveness measured for the sample with 18wt.% is around 15dB. These results are obtained with 4mm thick samples. The shielding effectiveness values can be further increased by increasing the sample thickness and/or the percentage of biochar. The shielding effectiveness of the plain cement composites decreases with frequency. This behaviour is similar to other cement

composites [34]. The different behaviour in frequency of the biochar composites with respect to plain cement composites can be attributed to the presence of entrapped water in the biochar [35].

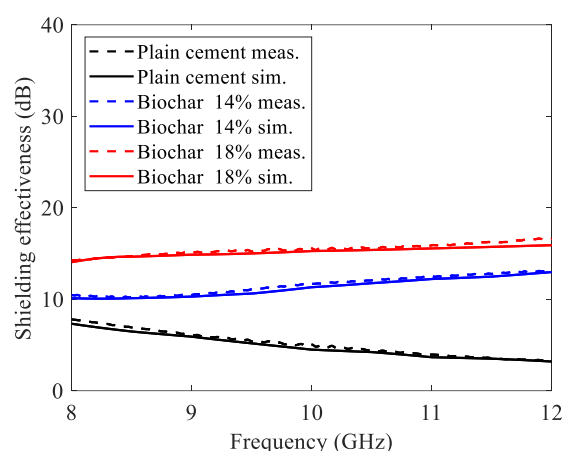


Figure 7. Measured and simulated Shielding effectiveness values for plain cement, sample with 14wt.% of biochar and sample with 18wt.%. Samples cured for 7 days in water. Measurements performed after ten weeks ageing.

In Figure 7 the simulated shielding effectiveness obtained with full-waves simulations are reported (dashed lines). The values of complex permittivity are varied to fit the simulated shielding effectiveness values to the measured shielding effectiveness values and a good correlation between the measured and simulated data is obtained.

There is a strong correlation between the curing period in water and the mechanical strength of cement composites [30]. In order to evaluate the effect of the curing period in water on the shielding effectiveness values, samples with 18wt.% biochar cured in water for a period of 7 days and 28 days are analysed. The shielding effectiveness of the cement composite with 18wt.% biochar cured in water for seven days and 28 days measured after 2 weeks and 10 weeks are shown in Figure 8. It can be seen that the sample cured in water for 28 days has higher shielding effectiveness when measured both after 2 weeks and 10 weeks. The variation of the shielding effectiveness over time of the cement composite cured for 28 days is also higher than the one cured in water for seven days. This shows that the shielding effectiveness is increased due to the presence of water, the loss of water from the sample over time results in a reduced value of the shielding effectiveness value.

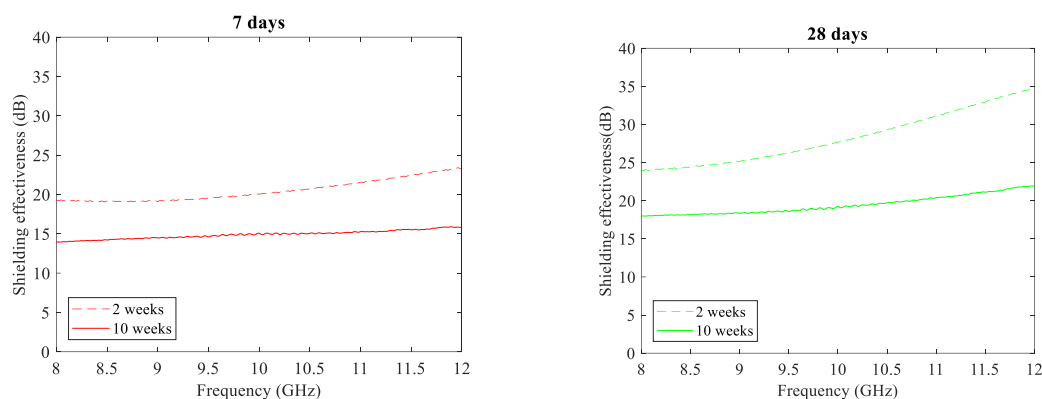


Figure 8. Measured shielding effectiveness of cement sample with biochar 18wt. % cured in water for 7 days (left panel) and 28 days (right panel). Measurements performed after 2 weeks and 10 weeks.

4. Discussion

In order to evaluate the impact of the presence of biochar in the cement composites on the shielding effectiveness, a comparison has been performed with other works in literature (see Table 2). The case considered in this comparison is filled with 18wt.% biochar cured in water for 7 days and measured after ten weeks. The thickness of the samples considered is 4mm which provide a shielding effectiveness value of almost 14dB. In comparison with literature, other cement samples reported gives higher shielding effectiveness values due to a higher value of thickness. In order to evaluate the impact of the thickness on the shielding effectiveness values, simulations are performed with higher thickness values. The results are shown in Figure 9. As expected the shielding effectiveness increases considerably increasing the thickness of the sample.

Table 2. Comparison with literature

Ref.	Frequency	Measured after (days)	Thickness (mm)	Shielding effectiveness (dB)	Materials
[34]	3 GHz	36	100	17.5	cement
[36]	10 GHz	95	150	20	cement
This work	10 GHz	70	4	15	cement+18wt.% biochar

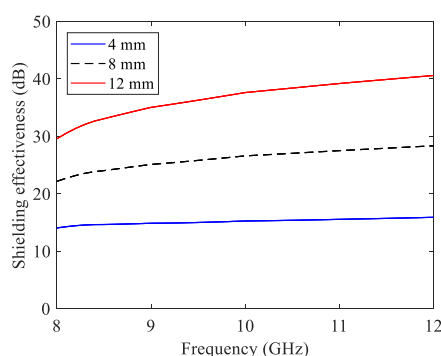


Figure 9. Simulated results for cement composites with 18wt.% biochar with different thicknesses.

5. Conclusions

Biochar is obtained by thermal treatment of waste products. It has been vastly used for soil amendment. More recently, it has been used for applications as energy storage, carbon sequestration and construction. The effect of a commercial biochar on the shielding properties of cement composites is investigated in X-band. The conclusions drawn based on the results presented can be extended to other microwave frequencies. Cementitious composites with ordinary Portland Cement (PC) were prepared without biochar and with biochar as filler (14 wt.% and 18wt.%). Samples are prepared in order to fit a WR90 waveguide (8-12 GHz). With the help of a full-wave simulator, the fabrication tolerances of the samples are analysed. A variation of $\pm 0.5\text{mm}$ results in a change of the shielding effectiveness of $\pm 1\text{dB}$. Shielding effectiveness can be obtained from the measurements of scattering parameters. Samples with 14wt.% and 18wt.% biochar as filler are cured in water for 7 days. As expected the shielding effectiveness increases with the increase of the percentage of filler (11dB for 14wt.%, and 15dB for 18wt.% at 10GHz). In order to evaluate the effect of the curing period in water on the shielding effectiveness values, different curing period are analysed. Samples with 18wt.% biochar are cured in water for a period of 7 days and 28 days. The shielding effectiveness increases by approximately 5dB in the whole frequency range for the samples cured in water for 28days as compared to samples cured in water for 7 days.

Author Contributions: composites fabrication, D.D., and G.R. ; waveguide measurements and discussion of the shielding effectiveness, D.D, M.Y. and P.S; microstructure characterization and TGA, I.N.S.; full-wave simulations, M.Y; original draft preparation, M.Y. and P.S.; writing—review and editing M.Y. , P.S. and I.N.S.; supervision, P.S.; conceptualization M.Y., P. S. and I.N.S., funding acquisition G.R. All authors have read and agreed to the published version of the manuscript.

Funding: This research received no external funding

Acknowledgments: The authors would like to thank Dr. Renato Pelosato for TGA measurements.

Conflicts of Interest: The authors declare no conflict of interest.

References

1. Klee, H.; Briefing: The Cement Sustainability Initiative. *Proceedings of the Institution of Civil Engineers - Engineering Sustainability* **2004**, *157* (1), 9-11.
2. Oh, D.-Y.; Noguchi, T.; Kitagaki, R.; Park, W.-J. CO₂ emission reduction by reuse of building material waste in the Japanese cement industry. *Renew. Sust. Energ. Rev.* **2014**, *38*, 796–810.
3. Balasubramanian, J.; Gopal, E.; Periakaruppan, P. Strength and microstructure of mortar with sand substitutes. *Graevinar* **2016**, *68*, 29–37.
4. Van der Lugt, P.; Van den Dobbelsteen, A.A.J.F.; Janssen, J.J.A. An environmental, economic and practical assessment of bamboo as a building material for supporting structures. *Constr. Build. Mater.* **2006**, *20*, 648–656.
5. Klapiszewski, Ł.; Klapiszewska, I.; Ślosarczyk A.; Jesionowski, T. Lignin-Based Hybrid Admixtures and their Role, *Cement Composite Fabrication, Molecules* **2019**, *24* (19), 3544.
6. Research and Markets. Available online: https://www.researchandmarkets.com/research/6mzxvg/microwave_devices (accessed on 25 February 2020).
7. Delhi N.; Behari G. Electromagnetic pollution-the causes and concerns, Proceedings of International Conference of Electromagnetic Interference and Compatibility, Bangalore, India, 23 February, 2002.
8. McKerchar W. D. Electromagnetic Compatibility of High Density Wiring Installations by Design or Retrofit, *IEEE Trans on Elm. Comp.* **1965**, *7* (1), 1-9.

9. Wang Y.; Gordon S.; Baum T.; Su Z. Multifunctional Stretchable Conductive Woven Fabric Containing Metal Wire with Durable Structural Stability and Electromagnetic Shielding in the X-Band, *Polymers* **2020**, *12* (2), 1-15.
10. Lee, H.-S.; Park J.-h.; Singh, J.K.; Hyun-Jun Choi *et al.* Electromagnetic Shielding Performance of Carbon Black Mixed Concrete with Zn–Al Metal Thermal Spray Coating, *Materials*, **2020**, *13*(4), 1-16.
11. Mojtaba A.; Maryam, I.; Saripan, A.; Iqbal, M.; Hasan W. Z. W. Three dimensions localization of tumors in confocal microwave imaging for breast cancer detection, *Microwave and Optical Technology Letters* **2015**, *57* (12), 2917–2929.
12. Peng, K.-C.; Lin, C.-C.; Li, C.-F. *et al.* Compact X-Band Vector Network Analyzer for Microwave Image Sensing, *IEEE Sensors Journal*, **2019**, *9* (1), 3304-3313.
13. Hanada, E.; Watanabe, Y.; Antoku, Y.; Kenjo, Y.; Nutahara, H.; Nose, Y. Hospital construction materials: Poor shielding capacity with respect to signals transmitted by mobile telephones, *Biomedical Instrumentation & Technology* **1998**, *32* (5), 489-96.
14. Khushnood, R.A.; Ahmad, S.; Savi, P.; Tulliani, J.M.; Giorcelli, M.; Ferro, G.A. Improvement in electromagnetic interference shielding effectiveness of cement composites using carbonaceous nano/micro inerts, *Constr. Build. Mater.* **2015**, *85*, 208–216.
15. Holloway, C.L.; Hill D.A.; Ladbury, J.; Koepke, G.; Garzia, R., Shielding effectiveness measurements of materials using nested reverberation chambers, *IEEE Transactions on Electromagnetic Compatibility* **2003**, *45* (1), 350–356.
16. Jung, M.; Lee Y.-S.; Hong, S.-G., Effect of Incident Area Size on Estimation of EMI Shielding Effectiveness for Ultra-High Performance Concrete With Carbon Nanotubes, *IEEE Access*, **2019**, *17*, 183106-183117, DOI: 10.1109/ACCESS.2019.2958633
17. Tamburrano, A.; Desideri, D.; Maschio, A.; Sarto, S., Coaxial Waveguide Methods for Shielding Effectiveness Measurement of Planar Materials Up to 18 GHz, *IEEE Transactions on Electromagnetic Compatibility* **2014**, *56* (6), 1386–1395.
18. Valente, R.; Ruijter, C.D.; Vlasveld, D.; Zwaag, S.V.D; Groen, P., Setup for EMI Shielding Effectiveness Tests of Electrically Conductive Polymer Composites at Frequencies up to 3.0 GHz, *IEEE Access* **2017**, *5*, 16665 – 16675.
19. Rudd, M.; Baum, T.C.; Ghorbani, K., Determining High-Frequency Conductivity Based on Shielding Effectiveness Measurement Using Rectangular Waveguides, *IEEE Transactions on Instrumentation and Measurement* **2020**, *69*, 155 – 162.
20. Gupta, S.; Tai, N.H.; Carbon materials and their composites for electromagnetic interference shielding effectiveness in X-band, *Carbon* **2019**, *152*, 159–187.
21. Giorcelli, M.; Savi, P.; Yasir, M.; *et al.* Investigation of epoxy resin/multiwalled carbon nanotube nanocomposites behavior at low frequency. *Journal of Material Research*, **2014**, *30*, 101-107
22. Savi, P.; Yasir, M.; Giorcelli, M.; Tagliaferro, A. The effect of carbon nanotubes concentration on complex permittivity of nanocomposites. *Progress in Electromagnetic Research M*, **2017**, *55*, 203-209
23. Khan, A.; Savi, P.; Quaranta, S.; Rovere, M.; Giorcelli, M.; Tagliaferro, A.; Rosso, C.; Jia, C.Q. Low-Cost Carbon Fillers to Improve Mechanical Properties and Conductivity of Epoxy Composites. *Polymers* **2017**, *9*, 642,1-14.
24. Peterson S.C., Evaluating corn starch and corn stover biochar as renewable filler in carboxylated styrene butadiene rubber composites, *Journal of Elastomers & Plastics*, **2011**, *44* (1), 43–54.
<https://doi.org/10.1177/009524431141401>

25. Giorcelli, M.; Savi, P.; Khan, A.; Tagliaferro, A. Analysis of biochar with different pyrolysis temperatures used as filler in epoxy resin composites. *Biomass Bioenergy* **2019**, *122*, 466–471.
26. Bridgwater, A.V. Review of fast pyrolysis of biomass and product upgrading. *Biomass Bioenergy* **2012**, *38*, 68–94.
27. Khushnood, R.A.; Ahmad, S.; Savi, P.; Tulliani, J.-M.; Giorcelli, M.; Ferro, G.A., "Improvement in electromagnetic interference shielding effectiveness of cement composites using carbonaceous nano/micro inerts", *Construction and Building Materials*, **2015**, *85*, 208–216.
28. Ding, Y.; Liu, Y.; Liu, S.; Zhongwu Li, et. al., Biochar to improve soil fertility. A review, *Agronomy for Sustainable Development*, **2016**, *36*, 1–18.
29. Ngan, A.; Jia, C.Q.; Tong, S.-T. Production, Characterization and Alternative Applications of Biochar. *Production of Materials from Sustainable Biomass Resources*, Springer, **2019**, 117–151.
30. Gupta, S.; Kua, H.W.; Low, C.Y., Use of biochar as carbon sequestering additive in cement mortar, *Cem. Concr. Compos.* **2018**, *87*, 110–129.
31. Gupta, S.; Kua, H.W.; Pang, S.D., Effect of biochar on mechanical and permeability properties of concrete exposed to elevated temperature, *Construction and Building Materials* **2020**, *234*, 117338.
32. Savi, P.; Yasir, M. Waveguide measurements of biochar derived from sewage sludge. *IET Electronics Letters*, **2020**, *56* (7), 335–337.
33. Savi, P.; Cirielli, D.; di Summa, D.; et al. Analysis of shielding effectiveness of cement composites filled with pyrolyzed biochar, Proceedings of the 2019 IEEE 5th International forum on Research and Technology for Society and Industry (RTSI), Florence, Italy, September 2019, pp. 1–4.
34. Donnell, K.M.; Zoughi, R.; Kurtis, K.E., Demonstration of Microwave Method for Detection of Alkali–Silica Reaction (ASR) Gel in Cement-Based Materials. *Cement and Concrete Research*, **2013**, *44*, 1–7.
35. Mrad, R.; Chehab, G. Mechanical and Microstructure Properties of Biochar-Based Mortar: An Internal Curing Agent for PCC. *Sustainability* **2019**, *11*, 1–15.
36. Kharkovsky, S.N.; Akay, M.F.; Hasar, U.C.; Atis, C.D., Measurement and monitoring of microwave reflection and transmission properties of cement-based specimens. *IEEE Transactions on Instrumentation and Measurement*, **2002**, *51*(6), 1210–1218.



© 2020 by the authors. Submitted for possible open access publication under the terms and conditions of the Creative Commons Attribution (CC BY) license (<http://creativecommons.org/licenses/by/4.0/>).